J. Plasma Physics (2005), *vol.* 71, *part* 4, *pp.* 379–388. © 2005 Cambridge University Press
doi:10.1017/S0022377804003150 Printed in the United Kingdom

Visible continuum radiation in high-pressure argon and argon–mercury plasmas

K. T. A. L. BURM

Philips Research Aachen, Weisshausstrasse 2, 52066 Aachen, Germany
(karel.burm@gmx.net)

(Received 12 October 2003 and accepted 17 May 2004)

Abstract. The sources for continuum emission are investigated in the visible wavelength range for a high-pressure argon plasma as well as for a high-pressure argon–mercury plasma used for light application. The mechanisms responsible for the continuum emission depend differently on the pressure, the temperature and the ionization degree. By changing these conditions it is shown that one can modify the dominant continuum radiation mechanism.

Operational improvement of the high-pressure argon–mercury test lamp are considered with respect to the continuum spectrum in the visible wavelength range.

1. Introduction

Low-pressure argon–mercury based, high-intensity discharge (HID) arc lamps are widely used for lighting purposes [1]. Here, the high-pressure regime is often defined as pressures above atmospheric pressure, to distinguish the high-pressure regime from the low-pressure regime. In practice, 'low pressure' is typically referring to lower than 1 kPa.

To improve the efficiency of the electrical power input an option is to increase the pressure in an argon–mercury HID lamp to the high-pressure regime. Meanwhile, it is hoped that, at higher pressure, the continuum emission of argon–mercury plasma may contribute to the emission in the visible wavelength range when the design parameters of pressure and temperature are chosen well. Here we will discuss the influence of pressure and temperature (or power input) on the sources of continuum emission in a test lamp, considering the wavelength range 300–800 nm. Our test lamp in Fig. 1 is a MHN150 quartz vessel (volume 2.4 cm^3) filled at room temperature with 12 mg mercury and 400 mbar argon. The pressure inside a burning MHN test lamp (150 W) roughly equals 1×10^6 Pa (which is in the high-pressure regime). The lamp is burned in a vertical position showing axial symmetry. A similar symmetry cannot be observed when the test lamp is burned in a horizontal position.

2. Sources of continuum radiation

The continuum radiation considered here originates from free electrons colliding with atoms and ions. If the free electron remains free after the collision, we speak of a free–free collision. If a free electron is captured by an ion, we speak of a

https://doi.org/10.1017/S0022377804003150 Published online by Cambridge University Press

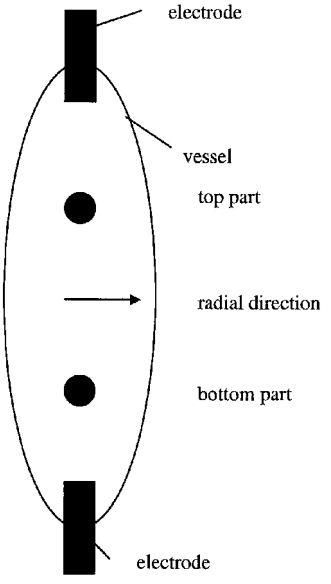


Figure 1. A schematic view of the vertically burned test lamp used. The black spots in the top and bottom parts of the lamp represent the measurement locations. The arrow indicates the radial direction.

free–bound collision or recombination collision. The radiation sources discussed here are known as Bremsstrahlung.

Indicating the type of radiation with a superscript and the colliding particles with subscripts, the emission coefficients ϵ of continuum radiation (the emitted power per unit of volume, solid angle and wavelength interval) are governed by the following expressions:

$$\epsilon_{\mathrm{ea}}^{\mathrm{ff}} = C_{\mathrm{ea}} \frac{n_{\mathrm{e}} n_{\mathrm{a}}}{\lambda^2} (kT_{\mathrm{e}})^{3/2} Q_{\mathrm{ea}}^{\mathrm{mom}} \left[\left(\frac{hc}{2\lambda kT_{\mathrm{e}}} + 1 \right)^2 + 1 \right] \exp\left(-\frac{hc}{\lambda kT_{\mathrm{e}}} \right), \tag{2.1}$$

$$\epsilon_{\mathrm{ei}}^{\mathrm{ff}} = C_{\mathrm{ei}} \xi_{\mathrm{ei}}^{\mathrm{ff}} \frac{n_{\mathrm{e}} n_{\mathrm{i}}}{\lambda^2} \frac{c}{\sqrt{kT_{\mathrm{e}}}} \exp\left(\frac{-hc}{\lambda kT_{\mathrm{e}}} \right), \tag{2.2}$$

$$\epsilon_{\mathrm{ei}}^{\mathrm{fb}} = C_{\mathrm{ei}} \xi_{\mathrm{ei}}^{\mathrm{fb}} \frac{n_{\mathrm{e}} n_{\mathrm{i}}}{\lambda^2} \frac{c}{\sqrt{kT_{\mathrm{e}}}} \left[1 - \exp\left(\frac{-hc}{\lambda kT_{\mathrm{e}}} \right) \right], \tag{2.3}$$

in which C_{ea} and C_{ei} are constants equal to [2–8]:

$$C_{\mathrm{ea}} = \frac{2}{3\pi^2} k_0^{2*} \alpha^3 a_0^2 \sqrt{\frac{2}{\pi m_{\mathrm{e}}}} hc = 2.0 \quad [\mathrm{W\ m^2\ J^{-3/2}\ sr^{-1}}], \tag{2.4}$$

$$C_{\mathrm{ei}} = \frac{1}{(4\pi\epsilon_0)^3} \frac{32\pi^2 e^6}{3\sqrt{3} c^3 (2\pi m_{\mathrm{e}})^{3/2}} = 2.023 \times 10^{-63} \quad [\mathrm{J^{3/2}\ m^3\ sr^{-1}}]. \tag{2.5}$$

The parameters k_0, α and a_0 are the wavenumber of the incoming electron, the fine structure constant of the atom and the Bohr radius of the atom, respectively:

$$k_0^2 = \frac{8\pi^2 m_{\mathrm{e}}}{h^2} E = k_0^{2*} E, \tag{2.6}$$

https://doi.org/10.1017/S0022377804003150 Published online by Cambridge University Press

$$\alpha = \frac{e^2}{2\epsilon_0 hc}, \tag{2.7}$$

$$a_0 = \frac{\epsilon_0 h^2}{\pi m_e e^2}. \tag{2.8}$$

Expression (2.1) is taken for the limit of zero photon energy [5]. According to Zollweg *et al.* [9] the limit of the zero photon energy method, or the asymptotic approximation method, often gives results correct to within about a factor of two. The method is most accurate for low electron energies E.

The parameters λ, T_e, n_e, n_i and n_a are the emitted wavelength, the electron temperature, the electron density, the ion density and the atom density, respectively. The constants h, k, ϵ_0, m_e, e and c are the Planck constant, the Boltzmann constant, the dielectric constant, the electron mass, the electric charge and the velocity of light, respectively. The parameters ξ_{ei}^{ff} and ξ_{ei}^{fb} are the free–free and the free–bound Biberman factors [10,11]. Although the Biberman factors are functions of the wavelength, the temperature and the ionization degree, they are usually close to one [4,7,12–16]. However, for short wavelengths (the visible range) the Biberman factor ξ_{ei}^{fb} deviates severely from one [12, 17, 18].

The Bremsstrahlung cross section, Q_{ea}, for electron–atom continuum radiation is set equal to the polarization cross section of the electron–atom collisions [3, 19, 20]. Note that the Bremsstrahlung cross section, Q_{ea}, is linear related to the cross section for the momentum Q_{ea}^{mom}. It is further assumed that the cross section for the momentum Q_{ea}^{mom} can be determined by taking the average electron energy [4]. For the quantitative approximations of the several emission coefficients we refer to [2–4, 12–15, 19, 21–23].

Furthermore, the total continuum radiation coefficient equals

$$\epsilon_{cont} = \epsilon_{ea}^{ff} + \epsilon_{ei}^{ff} + \epsilon_{ei}^{fb}. \tag{2.9}$$

Note that (2.2) and (2.3) have the same coefficient C_{ei} and can be combined to form the total electron–ion emission coefficient

$$\epsilon_{ei} = C_{ei}\xi_{ei}\frac{n_e n_i}{\lambda^2}\frac{c}{\sqrt{kT_e}}, \tag{2.10}$$

where ξ_{ei} is the total electron–ion Biberman factor.

To estimate the relative importance of continuum radiation from electron–atom collisions over those from electron–ion collisions the ratio R is introduced,

$$R = \frac{\epsilon_{ea}}{\epsilon_{ei} + \epsilon_{ea}} \tag{2.11}$$

(note that $\epsilon_{ea} = \epsilon_{ea}^{ff}$).

Indicating the division of the emission coefficients by $n_e n_x$ with an f_{ex} (with $x = a, i$) R becomes

$$R = \frac{f_{ea}}{\alpha f_{ei} + f_{ea}}, \tag{2.12}$$

with α the ratio of the ion density and the atom density (n_i/n_a).

Note that the functions f are only functions of the wavelength and the electron temperature. The ratio R is hence determined for each wavelength by the electron temperature and the ionization degree α. Furthermore, an advantage of discussing the emission ratio R over the absolute emission is that no (accurate) absolute calibration is required before analytic information can be obtained.

https://doi.org/10.1017/S0022377804003150 Published online by Cambridge University Press

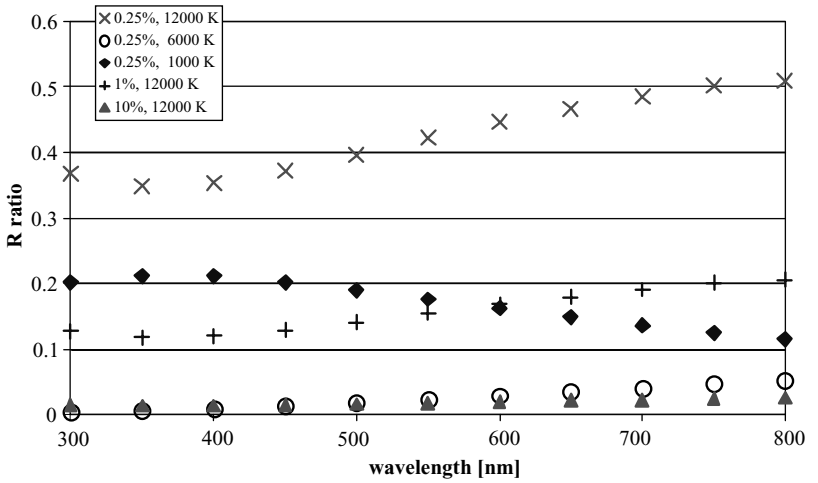


Figure 2. Tuning the dominant continuum radiation process (argon plasma).

3. Results

To reduce complexity, we will first discuss how to tune the visible continuum emission spectrum in argon plasmas. With argon plasmas we have a better reference literature than with argon–mercury plasmas for light applications. The principles are basically the same in both plasmas.

3.1. Tuning the dominant continuum emission processes in an argon plasma

In the previous section it was found that R is determined for each wavelength by the electron temperature and the ionization degree. In Fig. 2 some examples are given of how the dominant continuum radiation process (the ratio R) can be tuned for an argon plasma. In these figures the electron–ion Biberman factor ξ_{ei} is taken from [15]. As expected, the electron–ion continuum emission contribution increases (R decreases) when the ionization degree increases. The relation between the dominant continuum radiation process and the electron temperature is not as straightforward, as is shown in Fig. 3. For temperatures higher than 2000 K, R increases with the electron temperature. It is further interesting to note that the change does depend on the specific wavelength under consideration.

Figure 3 shows a 'peak' for the 1000–2000 K temperature range. To show the peak better, the resolution is increased for the 400 nm wavelength example. The peaks are due to the

$$\left[\left(\frac{hc}{2\lambda kT_{\mathrm{e}}}+1\right)^2+1\right]$$

term in the electron–atom emission coefficient, which decreases as a function of the wavelength and the electron temperature. The peak is therefore higher for shorter wavelengths and is located at 1500–2000 K.

The result for $\alpha = 0.25\%, T_{\mathrm{e}} = 12000$ K in Fig. 2 is somewhat lower than the result from de Regt et al. [21]. This is due to the difference in electron–atom Bremsstrahlung cross section. De Regt et al. assume that the Bremsstrahlung cross section can be set equal to the (momentum) impact cross section (the so-called billiard balls type approximation), while in our derivation the Bremsstrahlung

https://doi.org/10.1017/S0022377804003150 Published online by Cambridge University Press

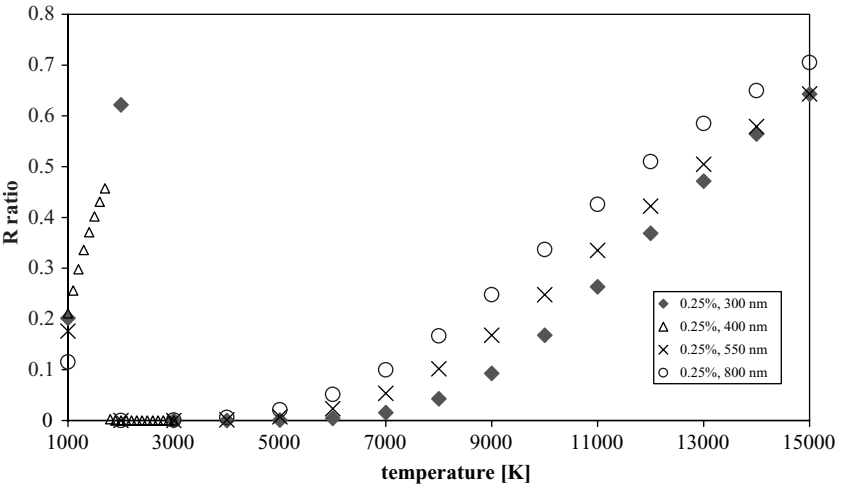


Figure 3. The dominant continuum radiation process as a function of the temperature (argon plasma).

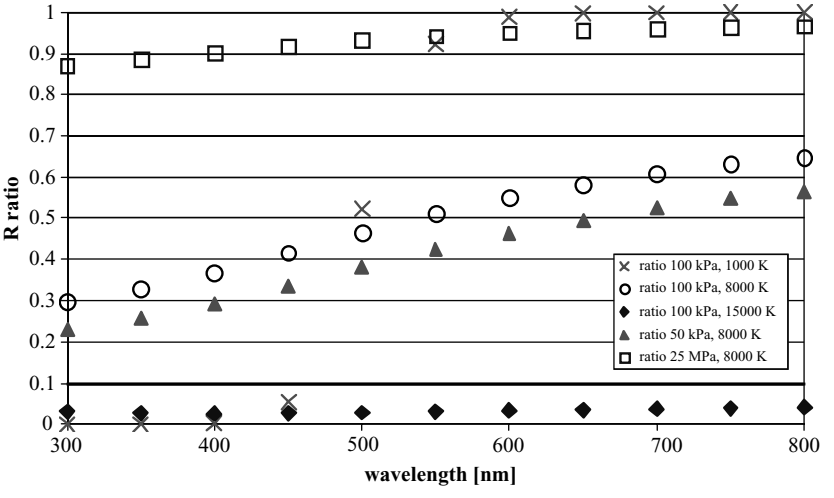


Figure 4. Tuning the dominant continuum radiation process (pressure and temperature) (argon plasma).

cross section was set equal to the cross section for electrons which collide with the polarization of the atom. This cross section is, however, linear with the impact cross section [6]. Therefore, the found behaviour of R as a function of the wavelength (e.g. a minimum at roughly 375 nm) should be identical, which is indeed found.

It is noted that it seems as if the dominant continuum radiation process is not determined by the pressure p. The ratio R is, however, a function of the pressure. Note that, by stating the ionization degree and the electron temperature, the ratio of pressure and atom density is given by

$$\frac{p}{n_{\mathrm{a}}} = (1 + 2\alpha)kT_{\mathrm{e}}.$$

https://doi.org/10.1017/S0022377804003150 Published online by Cambridge University Press

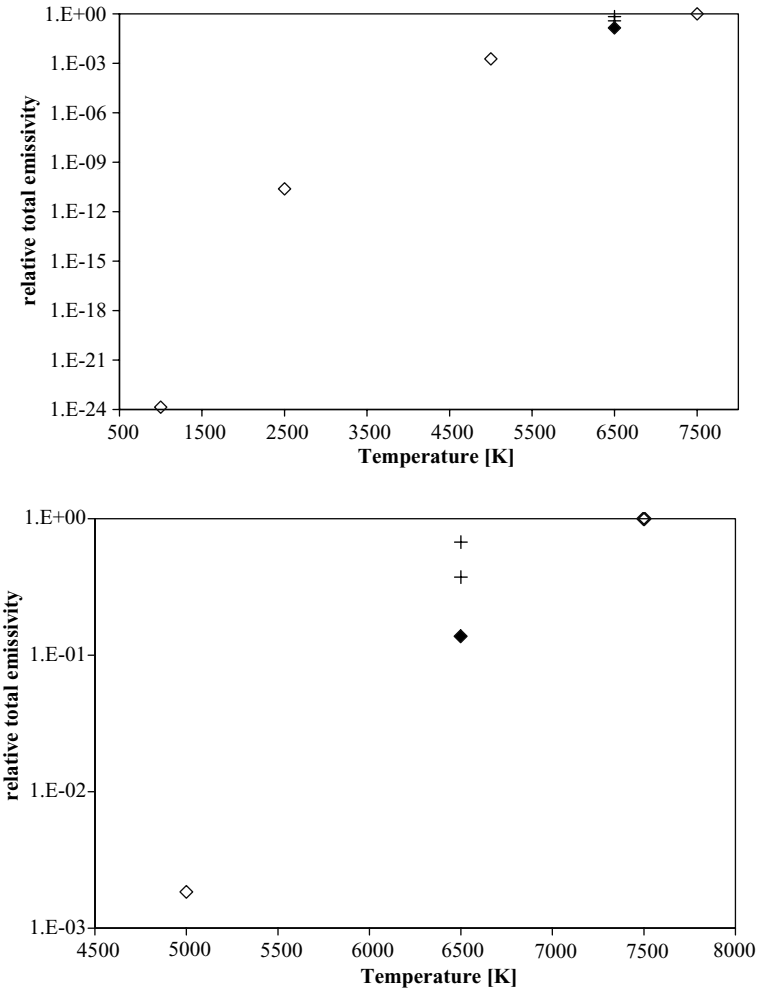


Figure 5. Increasing the temperature (triangles) or the pressure (crosses) inside the argon–mercury test lamp plasma. Shown is the ratio of the emissivity at 550 nm and its maximum at 7500 K.

Assuming local thermal equilibrium (LTE) the atom density is found from the Saha relation

$$\alpha^2 n_a = S(T_e) = \frac{2g_i}{g_a}\left(\frac{2\pi m_e k T_e}{h^2}\right)^{3/2} \exp\left(-\frac{E^{ion}}{kT_e}\right), \tag{3.1}$$

with g_i and g_a the statistical weights of the ion and the atomic ground state and E^{ion} the ionization energy. Therefore, by stating the ionization degree and the electron temperature the pressure is determined. Putting it differently, the dominant continuum radiation process is determined by two of the following three parameters: pressure, electron temperature and ionization degree. According to Figs 2–4, an increase in electron temperature (when the temperature is already higher than 2000 K) and pressure or a decrease in ionization degree, increases the importance of the electron–atom continuum radiation process.

https://doi.org/10.1017/S0022377804003150 Published online by Cambridge University Press

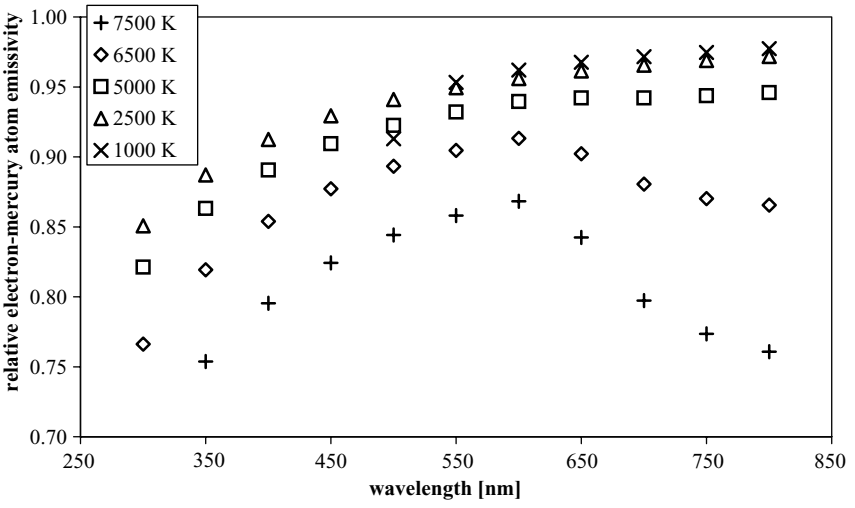


Figure 6. Increasing the temperature inside the argon–mercury test lamp plasma. Shown is the ratio between the electron–mercury atom, free–free Bremsstrahlung and the total emissivity for the visible spectrum.

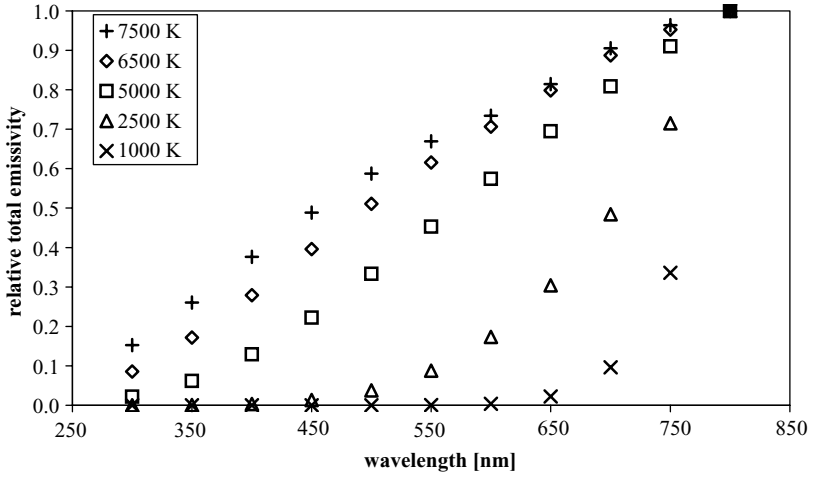


Figure 7. Increasing the temperature inside the argon–mercury test lamp plasma. Shown is the ratio of the total continuum emissivity and its maximum at 800 nm.

3.2. Tuning the dominant continuum emission processes in the test lamp

Here we will discuss the visible continuum spectrum of the argon–mercury test lamp plasma when we increase the temperature or the pressure. The Biberman factors for argon are taken from [15] and those for mercury are taken from [7].

In principle, an increase in temperature as well as an increase in pressure increases the emissivity over the total visible spectrum. We show in Fig. 5 how the emission at 550 nm is relatively influenced by temperature and pressure.

The emissivity behaviour of the test lamp is completely dominated by the mercury atoms, as shown in Figs 6 and 8. Although the maximum of the relative

https://doi.org/10.1017/S0022377804003150 Published online by Cambridge University Press

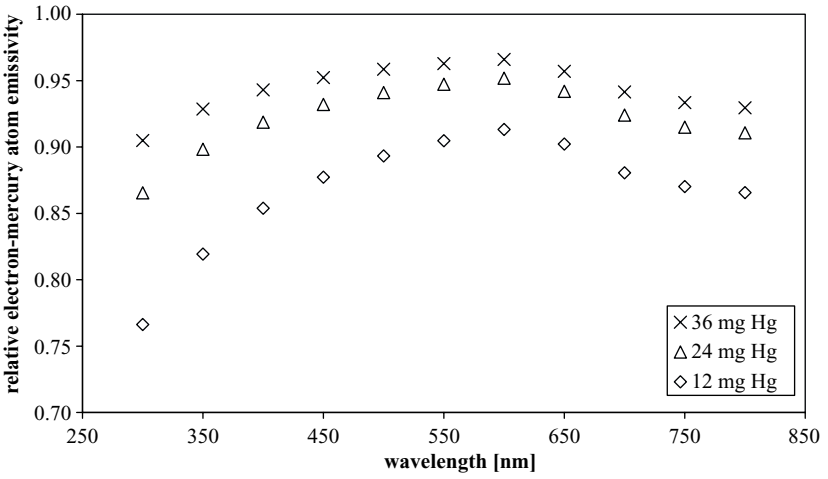


Figure 8. Increasing the pressure inside the argon–mercury test lamp plasma by increasing the mercury gas filling. Shown is the ratio between the electron–mercury atom, free–free Bremsstrahlung and the total emissivity for the visible spectrum.

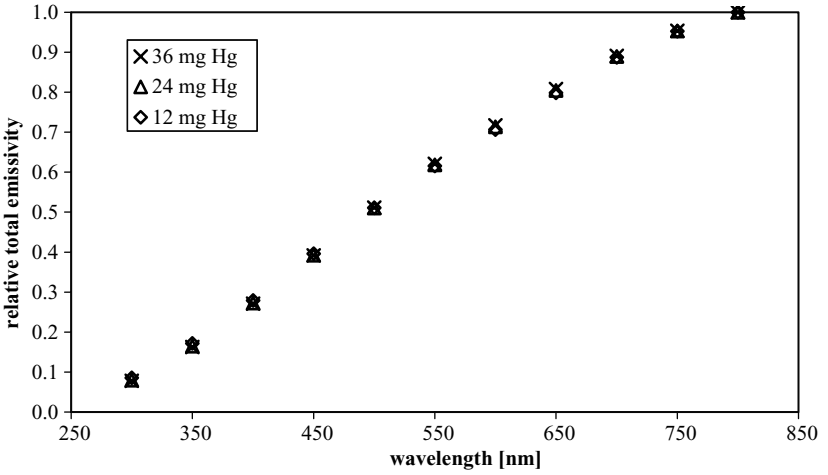


Figure 9. Increasing the pressure inside the argon–mercury test lamp plasma by increasing the mercury gas filling. Shown is the ratio of the total continuum emissivity and its maximum at 800 nm.

electron–mercury atom, free–free Bremsstrahlung emission coefficient, in Fig. 6, moves towards shorter wavelengths when the temperature increases, we do not observe such a behaviour for the relative total emission, in Fig. 7. Nevertheless, increasing the temperature improves the colouring of the visible emission according to both figures. It is the other Bremsstrahlung mechanisms (mainly electron–argon atom, free–free Bremsstrahlung at relative low temperatures of 1000–5500 K, and electron–mercury ion, free–bound Bremsstrahlung at relative high temperatures of 6500–7500 K) which cause the red 750–800 nm range to remain dominant in Fig. 7.

Increasing the pressure by increasing the mercury gas filling does not lead to an improved colouring according Fig. 9, although the maximum of the relative

https://doi.org/10.1017/S0022377804003150 Published online by Cambridge University Press

electron–mercury atom Bremsstrahlung moves towards lower wavelengths when the pressure is increased (Fig. 8). This maximum in Fig. 8 is not so evident as in Fig. 6. Furthermore, electron–mercury ion, free–free Bremsstrahlung and electron–mercury ion, free–bound Bremsstrahlung become important at the red side of the spectrum. They favour the red side of the spectrum more specifically than does the electron–argon atom, free–free Bremsstrahlung.

4. Concluding remarks

The visible continuum spectrum of argon plasmas and argon–mercury plasmas and the sources of the continuum radiation (Bremsstrahlung) were discussed here. We are interested in the continuum spectrum of argon–mercury plasmas for light applications, rather than Bremsstrahlung in argon plasmas as is more often studied in the literature. It was shown how one can tune the sources of continuum radiation as well as change the colouring of the argon–mercury plasma test lamp.

Since the plasmas discussed have typically high electron temperatures but low ionization degrees, the contribution of electron–atom continuum emission in the total continuum emission cannot be neglected. It is concluded that the test lamp performs better at higher temperatures, since the maximum of the electron–mercury atom, free–free Bremsstrahlung moves towards shorter wavelengths, while the total emission is increased. The influence of an increase in pressure is similar but much less effective.

One way to increase the temperature is to operate the test lamp at higher input powers. The size of the lamp vessel could be increased to keep low temperatures at the vessel walls.

Acknowledgements

The work presented here was performed while the author was a Marie Curie Industrial Host Fellow within the Research Framework ‘Improving Human Research Potential and the Socio-economic Knowledge Base’ of the European Union at the Philips Research Laboratories in Aachen, Germany. The work is financed by the European Commission Directorate Research of the European Union, Brussels.

References

[1] Elenbaas, W., de Boer, J. B., Hehenkamp, Th., Meyer, Chr., Tol, T., Wanmaker, W. L. and van de Weijer, M. H. A. 1966 Quecksilberdampfhochdrucklampen. Philips Technische Bibliothek, Eindhoven.

[2] Rutscher, A. and Pfau, S. 1968 *Beitraege Plasmaphysik* **8**, 315.

[3] Atajew, A., Rutscher, A. and Winkler, R. 1972 *Beitraege aus der Plasmaphysik* **12**, 239.

[4] Cabannes, F. and Chapelle, J. C. 1971 *Reactions under Plasma Conditions* (ed. M. Venugopalan). New York: Wiley.

[5] Mjolsness, R. C. and Ruppel, H. M. 1966 *Phys. Rev.* **154**, 98.

[6] Kasyanow, W. and Starostin, A. 1965 *Sov. Phys.–JETP* **21**(1), 193.

[7] Lochte-Holtgreven, W. 1995 *Plasma Diagnostics*. New York: American Institute of Physics Press.

[8] Thorne, A., Litzen, U. and Johansson, S. 1999 *Spectrophysics*. Berlin: Springer-Verlag.

[9] Zollweg, R. J., Liebermann, R. W. and Burnham, R. 1977 *J. Quant. Spectrosc. Radiat. Transfer* **18**, 133–141.

https://doi.org/10.1017/S0022377804003150 Published online by Cambridge University Press

[10] Biberman, L. M. and Norman, G. E. 1960 *Opt. I Spetrosk.* **8**, 230.
[11] Biberman, L. M., Norman, G. E. and Ulyanov, K. N. 1961 *Opt. I Spetrosk.* **10**, 297.
[12] Schram, D. C. and van de Sanden, M. C. M. 1997 Inleiding Plasmafysica. Report 3P110, Eindhoven University of Technology, Eindhoven.
[13] Boulos, M. I., Fauchais, P. and Pfender, E. 1994 *Thermal Plasmas*. New York: Plenum.
[14] Born, M. 2000 Private communication. Philips Research Aachen, Germany.
[15] Wilbers, A. T. M., Kroesen, G. M. W., Timmermans, C. J. and Schram, D. C. 1991 *J. Quant. Spectrosc. Radiat. Transfer* **45**, 1.
[16] Benoy, D. A. 1993 Modelling of thermal argon plasmas. PhD thesis, Eindhoven University of Technology, Eindhoven.
[17] Lelevkin, V. M., Otorbaev, D. K. and Schram, D. C. 1992 *Physics of Non-equilibrium Plasmas*. Amsterdam: North-Holland.
[18] Schlueter, D. 1964 *Z. Astrophys.* **61**, 67.
[19] Rutscher, K. and Pfau, S. 1976 *Physica* **81C**, 395–402.
[20] Chittka, U. 1988 Private communication. Philips Research Aachen, Germany.
[21] de Regt, J. M., van Dijk, J., van der Mullen, J. A. M. and Schram, D. C. 1995 *J. Phys. D: Appl. Phys.* **28**, 40.
[22] Thrum, T. 1999 Numerische Modellierung gepulst betriebener Hochdruckentladungslampen. PhD thesis, Universitaet Fridericiana Karlsruhe, Karlsruhe.
[23] Manola, S. and Devic, S. 1991 *J. Quant. Spectrosc. Radiat. Transfer* **46**, 577.

https://doi.org/10.1017/S0022377804003150 Published online by Cambridge University Press